Coupled Systems Mechanics, *Vol. 15, No. 2 (2026) 173-192*
https://doi.org/10.12989/csm.2026.15.2.173

Techno-Press

Seismic behavior analysis of electrical substation system by frequency response curves

N. Srujana[1], Shakti P Jena*[2]

[1]*Structural Health Monitoring Division, KDM Engineers India Private Limited, Hyderabad, India*
[2]*Department of Mechanical Engineering, Amrita School of Engineering, Amrita Vishwa Vidyapeetham, Chennai, India*

(Received March 2, 2026, Revised April 18, 2026, Accepted April 30, 2026)

Abstract. A complete laboratory-based seismic testing is the ideal standard qualification method to determine the amplified response accelerations of the electric power utility equipment. As an alternative to the complete experimental procedures, an analytical methodology with partial experimentation is proposed to assess the structural performance prior to the seismic qualification experiments in the present analogy. The proposed approach is based on the free vibration tests conducted at manufacturing unit, an analytical study of acceleration transmissibility and phase shifts of individual modes of the structure. This method also focuses on understanding the state of the system at post resonance. Different types of substation equipment are analyzed for the dynamic response and a case study of 36 kV circuit breaker is presented in this work. Harmonic vibrations of 0.2 g ground accelerations applied to index the modal parameter i.e., damping ratios at corresponding natural frequencies. Force transmission and phase lag at individual modes of the system opposing random ground accelerations are computed. The plots of frequency response curves of majority of the tested substation equipment showed the response acceleration is low at higher frequency ratios. Also, the response acceleration is not influenced by damping of the structure in the region of high frequency ratios. The presented methodology reduces the experimental complexities in the laboratories and the final qualification can be done in single attempt.

Keywords: electric substation equipment; frequency response; harmonic vibrations; phase shift; seismic qualification

1. Introduction

Various power utility structures are in demand of estimating the withstand capacity of the system against earthquakes not only at higher accelerations but also minimum 0.1 g ground accelerations [1]. There is always a substantial need for protecting public structures and public utility facilities from inevitable natural calamities like earthquakes. Post-earthquake rescue and relief activities are directly linked with public utility facilities like power transmission lines and electric substations in order to maintain public safety during the life ordeal. Past earthquake data evidence the low efficiency of power supply lines subjected to seismic vibrations and the structures having fundamental frequencies with low damping value falls between the stipulated ranges of earthquake vibrations have a significant effect on acceleration amplification and bending

*Corresponding author, Assistant Professor, E-mail: shaktipjena@gmail.com

ISSN: 2234-2184 (Print), 2234-2192 (Online)

stresses. According to the qualification standards (IEEE Std. [24]), the seismic performance is demonstrated through various experimental testing procedures depending on the type of the equipment and site specifications. Equipment has to be qualified at one of three seismic levels (low, moderate, high), each level corresponds to increasing ground acceleration demands. The qualification process includes a two stage test: sine sweep (for dynamic characteristics) and sine beat (for structural response under controlled excitation), along with TRS enveloped RRS shake table tests for to simulate earthquake vibrations for certain equipment types. The shake table experiments are utilized to identify the acceleration amplifications. In both the test stages, the equipment must be mounted on the test platform and enveloped seismic signals must be given to the shake table so as at the base of the structure. The responses at required locations and natural frequencies are to be observed with the help of accelerometers and strain gauges. Further, the standard recommends seismic qualification of power transformer using the method of analysis. The provision illustrates the modeling and analysis of entire transformer bushing system using numerical methods. Shake table experiments are mandatory for porcelain bushing (alone) with the bushing support structure by inducing dynamic response determined from numerical evaluations at the base of the bushing, mounted on the transformer. For the equipment mounted on support structures, the ground accelerations are not allowed to amplify at the top of the support structure and top of the equipment more than 2.25 and 2.0 times.

Majority of the electric equipment passed experimental investigations under site specified conditions in the testing laboratories. Nevertheless, higher rated porcelain bushings have exhibited shear failures due to the variation in the thickness of porcelain bushing mounting base plate. Ground acceleration amplification factors are more for new substation installations than standard recommended values especially in the cases of instrument transformers and power transformers [2-5]. Dinh et al. [6] did experimental investigations on 1000 kVA cast resin- hybrid mold transformer using tri-axial shaking table tests. The dynamic characteristics such as fundamental frequency, damping ratio and acceleration time history response, dynamic modification factors (DAF) and relative movements are evaluated as per the specifications of International Code Council Evaluation Services Acceptance Criteria ICC-ES AC156. The results produced severe slippage of the spacers and failure of linked bolts between support element and middle element of steel truss. In addition, the maximum relative displacement of the equipment is surpassed the boundary limit mentioned by the Korean National Radio Research Agency (KNRRA). Wen et al. [7] have studied the interaction between main plant and the electrical equipment connected to the plant using experimental investigations and numerical analysis. The findings are clearly announcing the grater amplifications are observed for stronger ground motions. Common seismic performance of substation plant- electrical equipment interaction can be achieved by considering strong column- weak beam idealization, which reduces the higher responses at the column-ends. In some counties, seismic qualification of electric equipment using shake table tests is in elementary stage. Noman Ullah et al. [8] presented comprehensive study of seismic response of substation equipment in the earthquake prone area of Pakistan. 132kV surge arrester was tested for time depended moderate accelerations as per Pakistan Electrical and Telecom safety Code PETSAC-2014 and IEEE Std. 693-2005. Cao et al. [9] developed simplified approach for seismic risk assessment and prediction of nuclear power cabinets which are integral parts of nuclear power plants. Using the approach seismic risk is estimated as a combination of fragile curves (capacity using cumulative absolute velocity (CAV) analysis) of the system and demand curves of probabilistic maps. Response surface methodology is employed to validate the analytical electric cabinet model using experimentations. It is observed the electric cabinet model has exhibited

higher capacity values than the recommended factor of 0.27 g. Zhu [10], worked on shock absorption technology of porcelain elements of substation equipment 1000 kV surge arrester. Force-displacement curve of shock absorber and Bouc-wen model are compared. Using the shock absorbers, seismic responses of pillar type porcelain components are suppressed. It is also observed that the installation radius and yield force of the installed shock absorbers increase, their shock absorption efficiency gradually decreases. Mohammadi et al. [11] implemented a parametric study to improve the seismic design of the substation equipment support structures to match with the IEEE Std 693, 2006 [24]. The study is focused about restricting the maximum acceleration at the intersection point of substation equipment and support structure. Minimum stiffness ratio is obtained for different equipment- support structure assemblies using the IEEE seismic qualification tests. The support structures considered in the study guarantees the IEEE specification of dynamic amplification factor (DAF) not exceeding 2.25. Reliable framework is developed to account the uncertainties of various severe ground motions. Using the probability analysis of DAF exceeding 2.5 for different substation equipment-support assembly is found to be 4 to 9%. Choosing the appropriate combination of support structure and substation equipment greatly reduces the seismic failures.

Kopse et al. [12] validated the dynamic model of a Slovenian power system using WAMS approach. The model developed in their analogy was designed for the dynamic stability analysis of the system by considering the relevant local modes only. Orlandini et al. [13] conducted a case study on the dynamic performance of a new power system incorporated with a wind farm. Their study predicts an innovative proposal motorized by a wind firm along with gas turbine and Organic Rankine Cycle (ORC) modules. The primary objective of their work is to recognize the highest amount of wind power that can be accommodated in the system without disturbing the balance of the grid system. The results obtained from the study showed that with the inclusion of the ORC module, there is decrease in the frequency of oscillations and fuel consumptions of the system.

Zareei et al. [14] have carried out a case study on the seismic susceptibility of power substation paraphernalia by considering a 420Kv circuit breaker. They have performed a 3D finite element modeling along with the time history analysis for the circuit breaker and recommended the seismic multivariate fragility function for the proposed circuit breaker. The additional reliable seismic risk can be evaluated from the observation of the fragility surface. Thus, the failure probability of the power substation system is vulnerable to different peak ground velocity and thus predicts the actual utilization of the power system in seismic zone. Baghmisheh and Estekanchi [15] presented the influence of dynamic interaction between the response of high voltage electric substation and the liability of substation equipment. The fragility function of each equipment was produced in the developed system using incremental dynamic analyses followed by Monte Carlo simulation approach to estimate the accuracy of the generated fragility functions. They have observed that with the inclusion of connection parts in the developed model can appreciably adjust the fragility of equipment and the relative performance of susceptible equipment. Thus, the fragility functions due to which the interaction effects are reported can be applied to evaluate the seismic risk of substations constantly.

Later, Baghmisheh and Estekanchi [16] proposed an approach to quantify the uncertainties occupied in the seismic response of an electrical substation structure by considering ground movement and modeling unpredictability. The proposed method employed the endurance time method mechanism to forecast the response distribution of the structure in a very short span of time. They have compared the present results with their earlier work i.e., impact dynamic analysis

method and found to be one accessible one. This method provided a better tool widening the application of recital-based design in electrical substation structure with even handed computational cost. Moustafa and Mosalam [17] developed an exact finite element model of electrical substation porcelain post insulators. This study is focused to explore the behavior and seismic response of structure through comprehensive numerical simulation which reduce the experimental prerequisite test and thus optimize the potential design of electrical structure. Xie et al. [18] addressed a method to diminish the influence of seismic action on heavy functional components mounted on the top of post electrical components. They have developed a theoretical method based on the distribution parameter system by considering the effects of lumped mass and moment of inertia. The finite element analysis along with vibration shaking table experiment are also conducted using ultra high voltage bypass switch with wire rope by including the effects of viscous damping to authenticate the proposed theoretical model. The results obtained from the developed method showed that the moment of seismic response and deflection confirmed a strong linear law with the enhancement of the lumped mass, but with a trend of nonlinear of deceleration.

Gong et al. [19] developed a numerical approach to investigate the seismic fragility of long span sustaining frames in ultra-high voltage electrical substation. A novel multi-ASI seismic vulnerability mechanism named as N-MASI-SFAM has been proposed by considering orientation of the substation and strike of the fault zone. They have investigated an epicenter position-based approach to approximate the seismic risk. Fu and Sivaselvan [20] presented the nonlinear dynamics of stretchy conductor which communicate components in high voltage substations. The nonlinear dynamics of stretchy conductors that act as a function in the response of substation components to earthquake excitation, and illustrates them is significant in view of seismic protection of substation structure in codes of practice. By experimentation, they observed that great diversity of nonlinear dynamic behavior arises based on the excitation frequency, slack intensity, and amplitude which results considerable out of plane motion and heavy fatal conductor force. Ghasemi et al. [21] discussed the various mechanism of failure incorporating the origin of cause, identification and extrapolative, degradation, and the remaining useful life of the structure. They investigated the various process and techniques to predict the rate of failure and the involved factors. They also identified some novel challenges of equipment to estimate the failure rate. Arredendo et al. [22] developed a simple model to calculate the vibrant behavior of rigid bodies subjected to earthquake induced forces. They proposed a numerical approach to analyze the response of 3-dimenssional rigid bodies along with experimental method as a verified one. Fu et al. also [23] investigated the seismic and failure analysis of transmission towers by considering various ground uncertainties.

Lekshmi and Mini [15] developed a Multi Tuned Mass Damper (MTMD) system for high rise building structure to control the seismic and harmonic excitations. Their methodology was very useful to minimize the acceleration, displacement and shear response of base at higher natural frequency levels. Botic et al. [26] developed a numerical method to explore the consequences of soil-structure interaction on the seismic response of multistory building structure. Lee et al. [27] carried out a laboratory (shaking table) test to appraise and evaluate the seismic performance of molded transformers consumed in hydropower plants. Fereidooni et al. [28] developed mathematical followed by finite element expression for the vibration analysis of steel frame structure subjected to earthquake. Magdy et al. [29] formulated a methodical investigation to evaluate the seismic performance of RC structure by considering steel fuse coupled beams. Han et al. [30] focused their investigation on the seismic performance of isolated steel frame incorporating the effects of torsional ground motion. Shin et al. [31] formulated a numerical model

for the seismic performance analysis of reinforced concrete column with corroded rebars.

As far as the safety of substation equipment concerned, some of the researches have addressed the gap between laboratory test results and the standard specified acceleration amplification factors. Also, work has been done on implying standard recommended amplification factors to design substation equipment-support structure assemblies. Several methodologies are proposed to validate the analytical procedures using shake table experiments and to recognize the earthquake resistant capacity of the power utility systems. Furthermore, Seismic resistant devices such as anchoring systems and metal shock absorbers are introduced by way of reducing ground amplifications. However, the standard recommended experimental test procedures are ideal and often tedious rather more energy consuming and sometimes transporting the heavy equipment from manufacturing plant to the laboratory is cumbersome. In the absence of such testing facility estimating the influential dynamic parameters of the sample equipment for earthquake vibrations is highly difficult. Therefore, it is required to propose an alternative procedure to identify the seismic efficiency of the structure while reducing the testing complexities. In addition to that, identification of post resonance behavior is mandate task to control peak ground accelerations from inflowing to the structure as the equipment may experience higher amplifications leading to failure though it is designed for specified seismic loads, also design modifications can be done prior to field installations. Hence, analytical frequency response curves are proposed identify the post resonance behavior to avoid testing complexities where shake table testing is difficult.

The current study presents a case study for the analytical approach in identifying seismic responses using dynamic motion formulations and thereby frequency response curves. The analytical study is to incorporate transmissibility factor and phase angle through frequency response curves to an explicit derivation of response characteristics of the structure to the real-time random vibrations. Frequency response curves are drawn as amplitudes of response quantity depending on excitation frequencies. Although the objective is not to rule out the experimental procedure but to minimize the complexity involved in adjusting the sample equipment to the test bed and carrying out the experiments. Nevertheless, the basic dynamic parameters of the structure such as fundamental frequencies and damping ratios are identified using single frequency vibration tests. The proposed approach is implemented on different types of substation equipment –circuit breakers, current transformers and potential transformers. The detailed process of estimating the seismic response of 36 kV circuit breaker opened to zone V spectral values as per Indian Standard IS: 1893 [24] is presented in the paper.

2. Evaluation of steady state response characteristics of the continuous system

Steady state response of either continuous or discrete system apparently derives force transmission and the change in cyclic phase of the structure. Derivation to the performance characteristics from the application of non-linear vibrations at the support of the structure are dealt in a pragmatic approach. Analytical formulations of dynamic systems having continuously distributed mass and elasticity consists of partial differential equations which can predict exact solutions to the actual behavior of the system by generating the solution to the infinite number of coordinates using the infinite degrees of freedom. The response displacement solutions to the governing equations are expressed in terms of generalized coordinate $u(t)$ and shape function $\Psi(x)$. Hence the solution for response acceleration is,

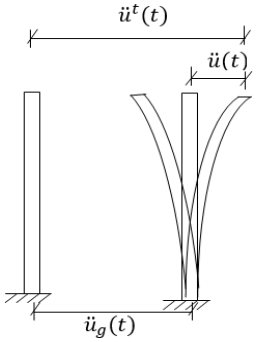

Figure. 1 Free body diagram of structural response at base excitation

$$u(x,t) = \psi(x)u(t)$$
$$u''(x,t) = \psi''(x)u(t)$$
$$\ddot{u}(x,t) = \psi(x)\ddot{u}(t)$$

In the case of the system with base excitation, the solution is derived in two steps- absolute motion of the support along with the super structure and relative motion of the top of the structure to the base of the support where ground vibrations are induced to the structure. Therefore, the ultimate response of the structure $\ddot{u}^t(t)$ is the combination of response at the top of the structure $\ddot{u}(t)$ and the response of the support motion $\ddot{u}_g(t)$.

$$\delta w_E = \delta u\left[\ddot{u}(t)\int_o^l m(x)\left(\psi(x)\right)^2 dx + \ddot{u}_g(t)\int_0^l m(x)\psi(x)dx\right]$$

$$\delta w_1 = \delta u\left[u(t)\int_o^l EI(x)\left(\psi''(x)\right)^2 dx + \delta u\int_0^l c(x)\psi(x)\dot{u}(t)dx\right]$$

$$\delta u = \left[\tilde{m}\ddot{u}(t) + \tilde{c}\dot{u}(t) + \tilde{k}u(t) + \tilde{L}\ddot{u}_g(t)\right] = 0, where$$

$$\tilde{m} = \int_0^L m(x)\left(\psi(x)\right)^2 dx, \tilde{k} = \int_0^L EI(x)\left[\psi''(x)\right]^2 dx, \tilde{c} = \int_0^L c(x)\left[\psi(x)\right]dx, \tilde{L} = \int_0^L m(x)\psi(x)dx$$

Therefore,

$$\ddot{u}(t) + \frac{\tilde{c}}{\tilde{m}}\dot{u}(t) + \frac{\tilde{k}}{\tilde{m}}u(t) = -\frac{\tilde{L}}{\tilde{m}}\ddot{u}_g(t)$$

$$\ddot{u}(t) + \frac{\tilde{c}}{\tilde{m}}\dot{u}(t) + \frac{\tilde{k}}{\tilde{m}}u(t) = \frac{F_0\sin\omega_0(t)}{\tilde{m}}$$

$$u(t) = \frac{F_0\sin\omega_0(t)}{\tilde{m}\left[D^2 + \frac{\tilde{c}}{\tilde{m}}D + \frac{\tilde{k}}{\tilde{m}}\right]}$$

From the solution of ordinary differential equation,

$$u(t) = \frac{F_0\sin(\omega_0 t - \phi)}{k\sqrt{(1-r^2) + (2\zeta r)^2}}$$

$$u(t) = \frac{-m\ddot{u}_g \sin(\omega_0 t - \phi)}{k\sqrt{(1-r^2) + (2\zeta r)^2}}$$

Here, $u(t)$ is the relative motion at top of the structure to the support base at the induced motion which is absolute motion of the structure. Altogether the total response of the structure is influenced by the relative motion from absolute motion of the structure in terms of ground acceleration $\ddot{u}_g(t)$

$$m\ddot{u}^t(t) + c\dot{u}^t(t) + ku^t(t) = ku_g(t) + c\dot{u}_g{}^t(t)$$

$$m\ddot{u}^t(t) + c\dot{u}^t(t) + ku(t) = 0$$

Substitute the relative motion $u(t)$ in the above expression and deriving total response of the structure,

$$\ddot{u}^t(t) = \frac{\sqrt{\left(1+(2\zeta r)^2\right)}}{\sqrt{\left(1-r^2\right)+\left(2\zeta r\right)^2}}\ddot{u}_g(t)\sin(\omega t - \phi - \phi_1) \tag{1}$$

$$\ddot{u}^t(t) = T_r\ddot{u}_g^t(t)\sin(\omega_0 t - \phi - \phi_1) \tag{2}$$

$$T_r = \frac{\sqrt{\left(1+(2\zeta r)^2\right)}}{\sqrt{\left(1-r^2\right)+\left(2\zeta r\right)^2}} \tag{3}$$

T_r is acceleration transmissibility factor is the ratio of the acceleration transmitted at the top of the structure to the max amplitude of the ground acceleration that the support base experience. It signifies the amplified value which is used to assess the behavior of the structure. The ratio of transmission is identical for force, acceleration, and displacement quantities. 'r' is the frequency ratio with forcing frequency to the fundamental frequency of the structure and 'ζ' is the damping ratio of the structure.

Phase angle (ϕ):

Phase is the distance (response) of a point that lags in an oscillation to its origin when compared to the input harmonic signal and is the parameter of time measured in degrees. In the case of base excitation, the response of the structure has phase shifts with the absolute motion and with the relative motion. If 'ϕ' is the phase angle with the top of the structure relative to the support movement and 'ϕ_1' is the phase angle with the support movement to the ground acceleration at the support.

$$\phi = Tan^{-1}\frac{\left(c\omega_0\right)}{\left(k - m\omega_0{}^2\right)} = Tan^{-1}\frac{\left(2\zeta r\right)}{\left(1-r^2\right)}$$

$$\phi_1 = Tan^{-1}\left(\frac{-c\omega_0}{k}\right) = Tan^{-1}\left(-2\zeta r\right)$$

Hence, 'ϕ^1' is phase angle with the response of the structure to the base excitation,

$$\phi^1 = \phi + \phi_1 \tag{4}$$

Therefore, the response shift of the structure is captured as a function of frequency ratio and modal damping factor using two phase angles ϕ and ϕ_1. Various power electric structures are

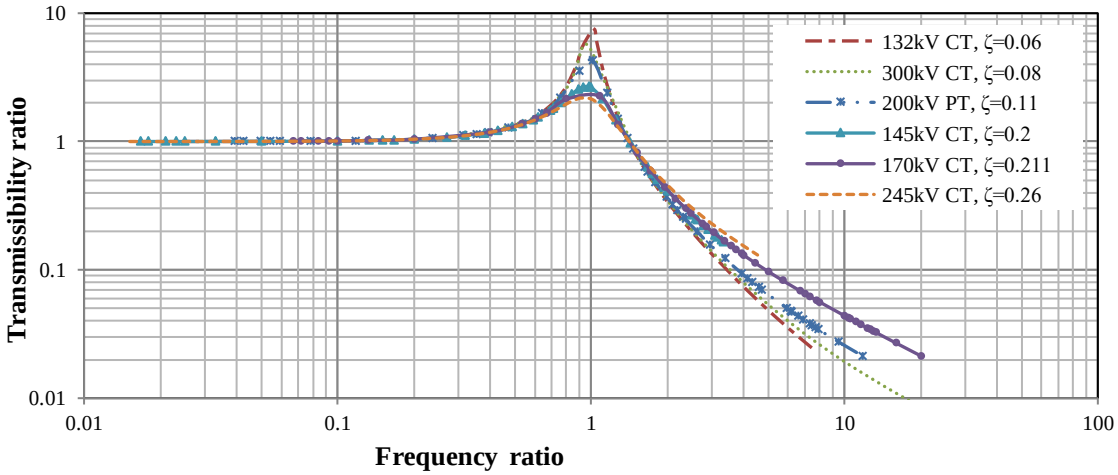

Figure 2(a). Frequency response curves of instrument transformers with varying damping values (*Tr* vs. *r*)

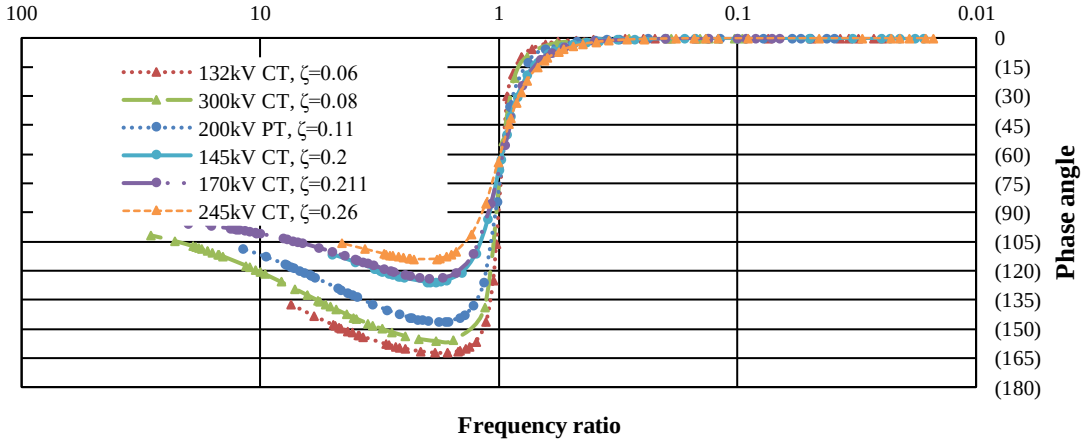

Figure 2(b). Frequency response curves of instrument transformers with varying phase angles (*Tr* vs. ϕ)

considered as examples of continuous systems due to distributed mass and elasticity. Moreover, the equipment is anchored on steel lattice towers of certain height depending on the substation productivity. Substation equipment of 132 kV Potential Transformer, 300 kV Current Transformer, 200 kV Potential Transformer, 145 kV-Current Transformer, 170 kV Current Transformer, 245 kV Current Transformer and 36 kV Circuit Breaker against seismic zone V design spectra are selected for the study.

The excitation-curves demonstrate the dynamic response characteristics such as enforced base transmission and the phase shift of the system. These curves consist of individual plots of transmissibility ratio (*Tr*) and phase angle (ϕ^1) with varying frequency ratios (*r*) at modal damping. The seismic performance against zone V design spectra of current transformer and potential transformer of different rating electrical substation corresponding damping values is given in frequency response curves of Fig. 2 (a) and (b). The joint observations are drawn for the multiple substation equipment based on the excitation-frequency curves. For all values of:

a) If $\left(\frac{\omega_0}{\omega_n}\right) \prec\prec\prec 1$, at lower excitation frequencies the ratio of transmission is approximately equals to1.0 irrespective of damping,

b) If $\left(\frac{\omega_0}{\omega_n}\right) \succ\succ\succ 1$, at higher levels of input frequencies the *T*of all systems is limiting to zero for any value of damping.

c) If $\left(\frac{\omega_0}{\omega_n}\right) \approx 1$, systems are sensitive to the damping and at low levels of damping, the transmitted acceleration is several times higher than the maximum amplitude of ground acceleration. Increment in damping reduces the response transmission at all forcing frequencies.

At maximum force transmission $f_T^0 \prec F_0$ (Applied force), response of the system is negligible almost equals to zero under the higher forcing signals. In another set of curves related to the phase angle versus frequency ratio, the phase shift is always meant to be negative.

a) If $\left(\frac{\omega_0}{\omega_n}\right) \prec\prec\prec 1$, phase angle ϕ^1 is close to 0° and independent of damping,

b) If $\left(\frac{\omega_0}{\omega_n}\right) \succ\succ\succ 1$, the response shift asymptotes to 180° for less damped systems,

c) If $\left(\frac{\omega_0}{\omega_n}\right) \approx 1$, represents peak response at ϕ^1=90°, which is in resonance for the least damped case. At higher levels of damping, the phase angle is less than 90° at resonance.

The implications of the above observations related to the system behaviour are explained in results and discussions.

2.1 Development of frequency response curves to substation equipment

The frequency response curves of a system are generated in couple of steps. a) identification of

Figure 3. 36 kV circuit breaker mounted on shake table

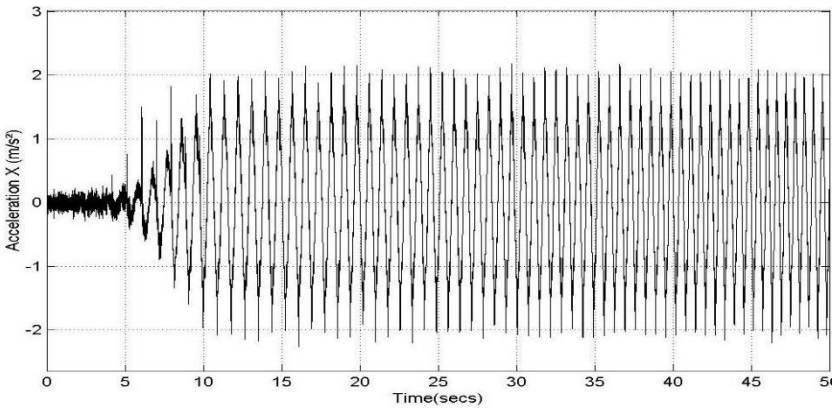

Figure 4. Time history of 0.2 g sine sweep acceleration in x-axis

fundamental dynamic parameters- fundamental frequency and modal damping using free vibration tests conducted at the field location or at the manufacturing unit, b) evaluating the response data of acceleration transmission as well phase angles at the corresponding frequency ratios, with the aid of the above formulations. Later, time history and response spectra of the system are estimated for predominant mode.

Case study of 36 kV circuit breaker:

Description of 36 kV circuit breaker: The total mass of the equipment is 480 kg. The circuit breaker has six insulators of height of 335 mm. The diameter of the insulator and wall thickness is 200 mm and 20 mm. Thickness of the insulator protection with rubber gaskets is 55 mm. The height of steel support truss is 1785 mm. The supporting structure is fabricated with mild steel angles. The vertical, horizontal, and bracing members are fabricated using angle section (65×65×6) mm. The bracing members are connected to the vertical main members using mild steel bolts of 16 mm diameter. The structure is mounted on two ISMC section making feasible to adjust on the shake table. The control cubical of size (840×300) mm was mounted on the supporting structure.

Test procedure: Sine sweep tests are conducted on the equipment using tri-axial shake table. Continuous sine sweep acceleration of 0.2 g with the sweep rate of 1 octave per minute is given as input to the shake table as shown in Fig. 4. The experimental test setup for the execution of modal tests may be shaking table or basic mechanical system (ex: harmonic tests, pullout tests); the vibration data could be of 0.1 g or free oscillatory data. The response acceleration and amplified response along with the fundamental frequencies can be obtained using FFT method. The response amplifications corresponding frequencies normalized from the response to the input excitation provided are shown in Fig. 8. Whereas simplified response (Fig. 8) is generated using transfer function, provides absolute responses by smoothening the local peaks. It is more realistic than the Fig. 7. Using FFT method, the input FFT shown in Fig. 5 has the highest amplitude noted as 16 m/sec^2 then the amplitude steps down accompanying multiple peaks as frequency forwards by indicating the peak accelerations at fundamental frequencies of the system. The scenario is confirmed in output FFT which is the resulting response of the system shown in Fig. 6. Thus, the amplified acceleration is estimated using the ratio of output FFT to input FFT. The FFT analysis is performed to verify the responses plotted from the transfer function. With the help of peaks and using half power bandwidth method, damping ratios at individual modal frequencies are obtained.

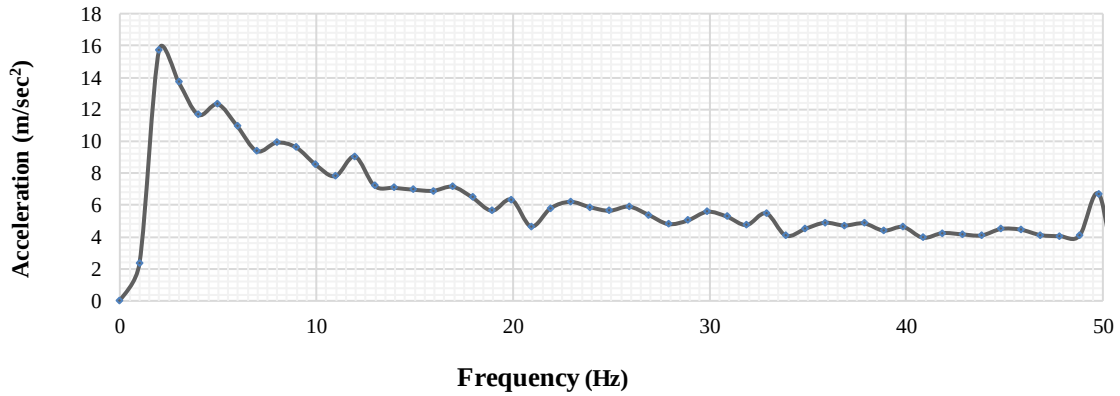

Figure 5. FFT of 0.2 g base acceleration in x-axis

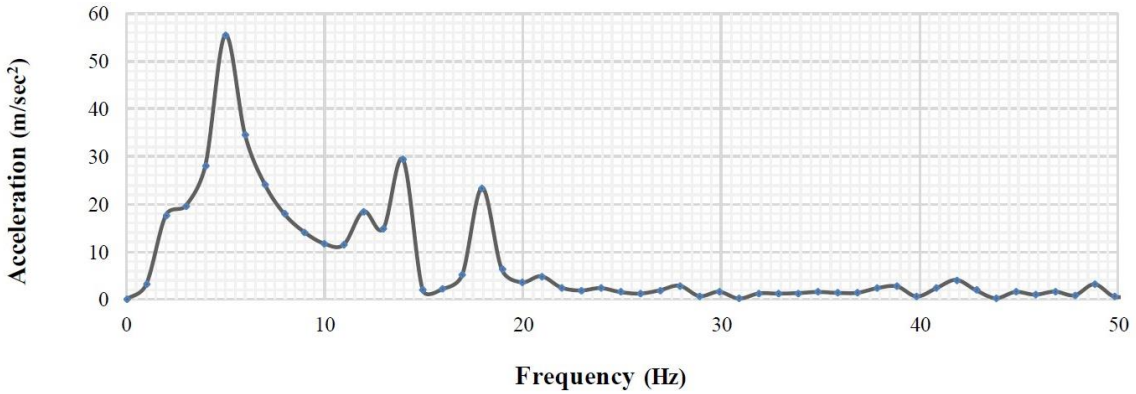

Figure 6. FFT of response acceleration at top of the equipment in x-axis

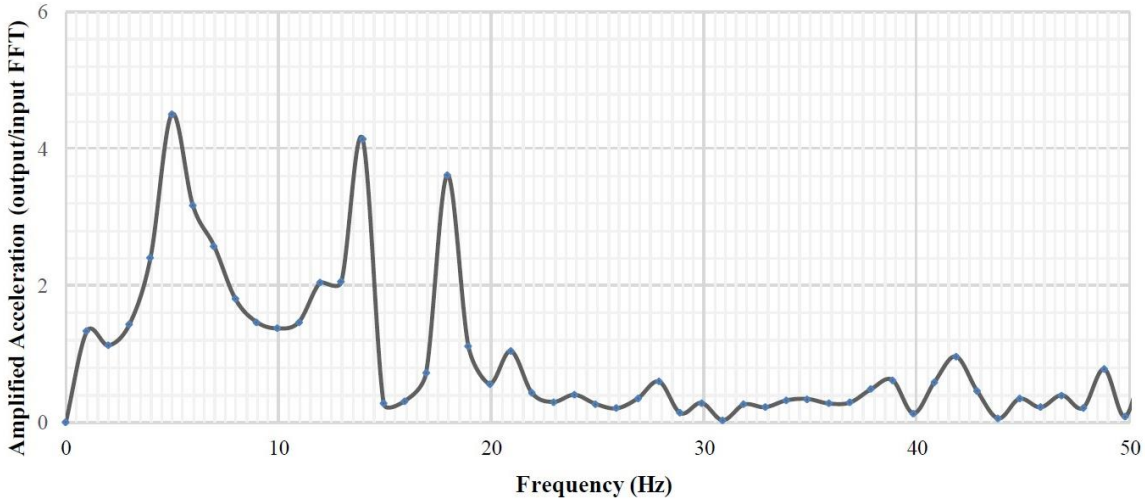

Figure 7. Amplified acceleration (output FFT/input FFT) at top of the equipment in X-axis

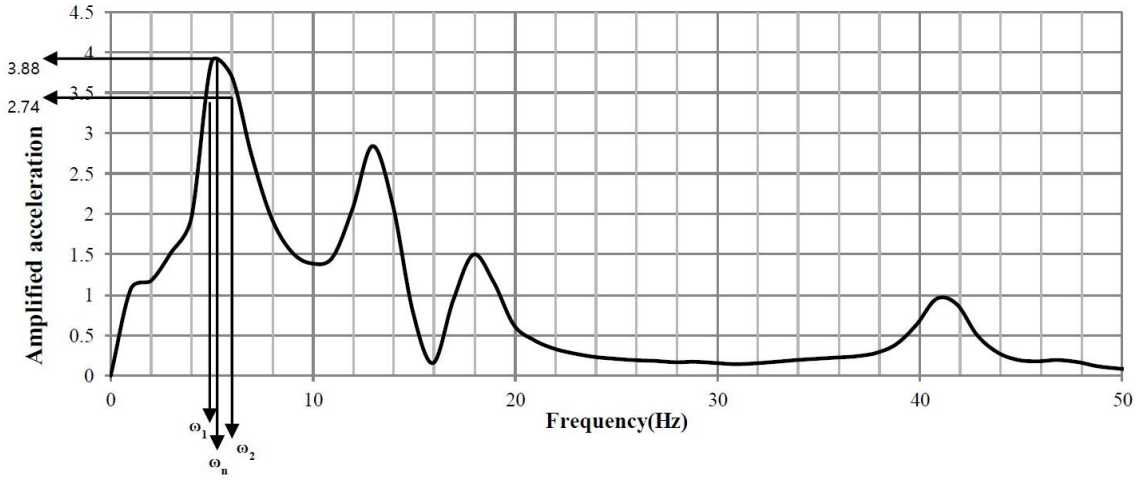

Figure 8. Calculation of damping using half power bandwidth method

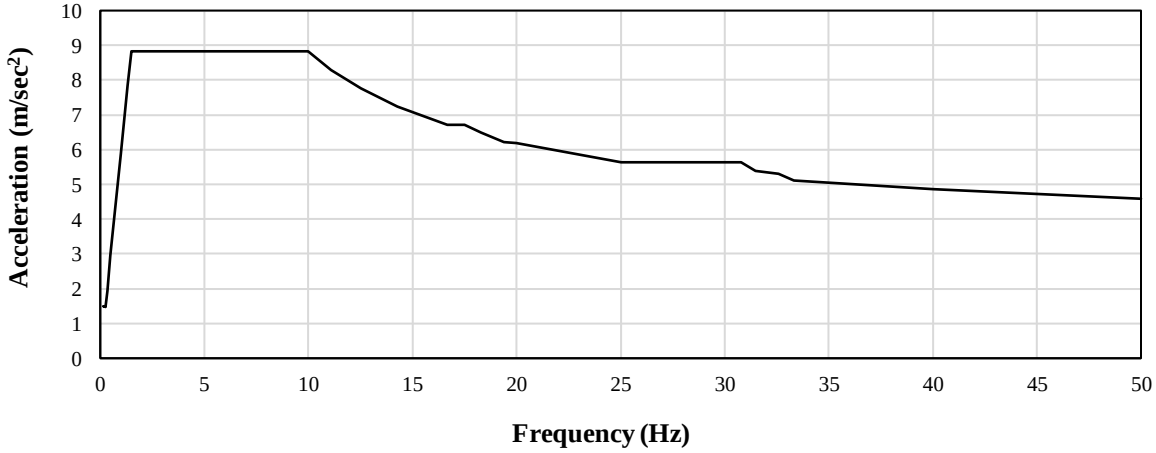

Figure 9. Zone V design spectra at 5% damping

Damping directly influences the amplification of seismic responses; low damping leads to higher amplification as fundamental frequency matches forcing frequency. Damping ratio is identified for the first mode of 36 kV circuit breaker from the plot of dynamic amplification vs. resonance frequency. Modal damping calculation for the first mode is shown in Fig. 8 and is depicted as 0.26. Similarly, the process is completed for rest of the modes individually.

$$\xi = \frac{\omega_2 - \omega_1}{2\omega_n} \tag{4}$$

The fundamental frequencies noticed are 4.98 Hz and 12.9 Hz in x-axis along with modal damping ratios 0.26 and 0.08. The steady state behavior of the system with the base excitation of zone V design spectra shown in Fig. 9 (as per IS: 1893-2016) is calculated using the amount of force transmission at top of the structure from the excited base which is at the base of the steel support structure i.e., *Tr* in Eq. (2) and the phase angle ϕ^1 of the system from ground acceleration

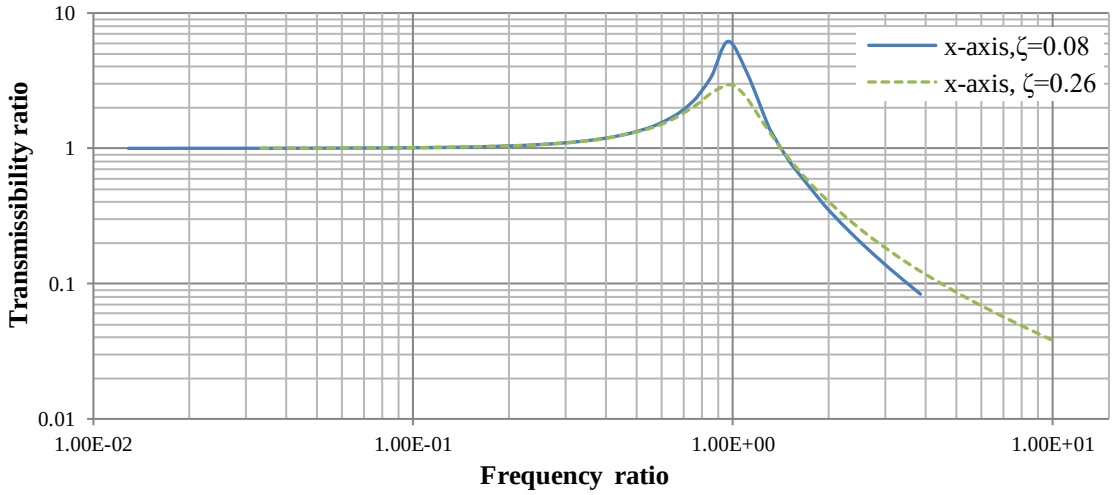

Figure 10. Frequency response curves of 36 kV-circuit breaker in x-axis (T_r vs. r)

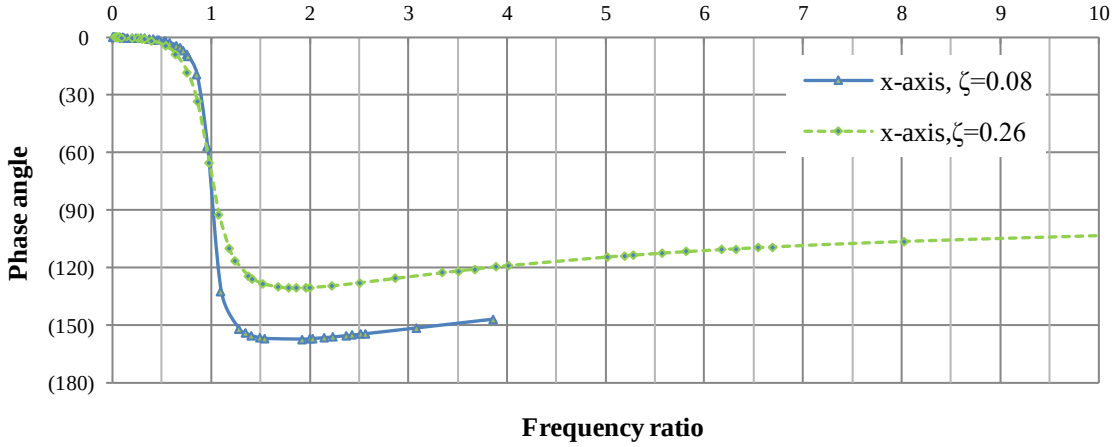

Figure 11. Frequency response curves of 36 kV-circuit breaker in x-axis ((ϕ^1) vs. r)

to the total response of the structure in Eq. (3). Two sets of frequency response curves connecting transmissibility ratio (T_r) vs. frequency ratio(r) and phase angle (ϕ^1) vs. frequency ratio (r) are outlined to the first modes in x, y axes are shown in Figs. 10 to 13. Time-dependent response accelerations at the top of the structure with the combination of absolute and relative motions of the equipment are calculated and are shown in Fig. 14. Design spectral values at 0.26 damping of fundamental mode against zone V ground acceleration data are plotted in Fig. 15. A MATLAB program flowchart (Fig. 16) is developed to calculate structural damping ratios using experimental free vibration tests. With the given earthquake data, the code develops frequency response curves and phase shift curves and produces the response time histories of the structure.

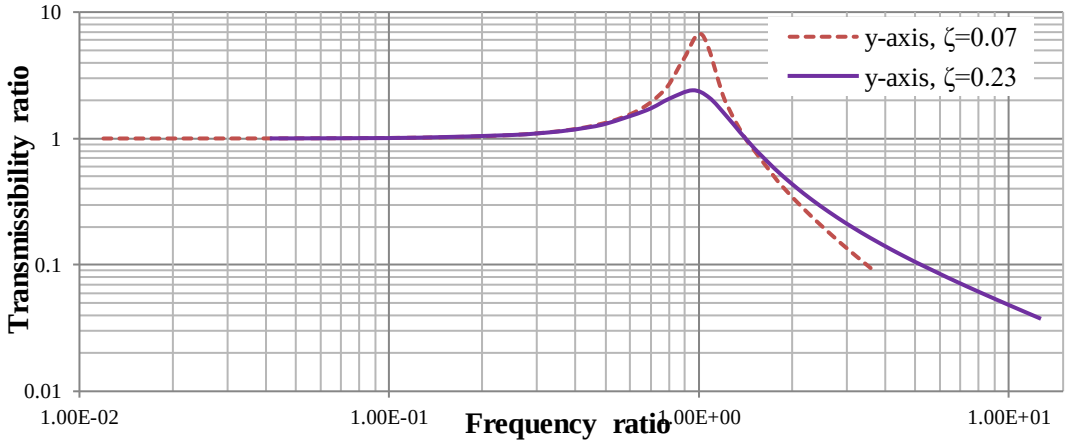

Figure 12. Frequency response curves of 36 kV-circuit breaker in x-axis ((ϕ^1) vs. r)

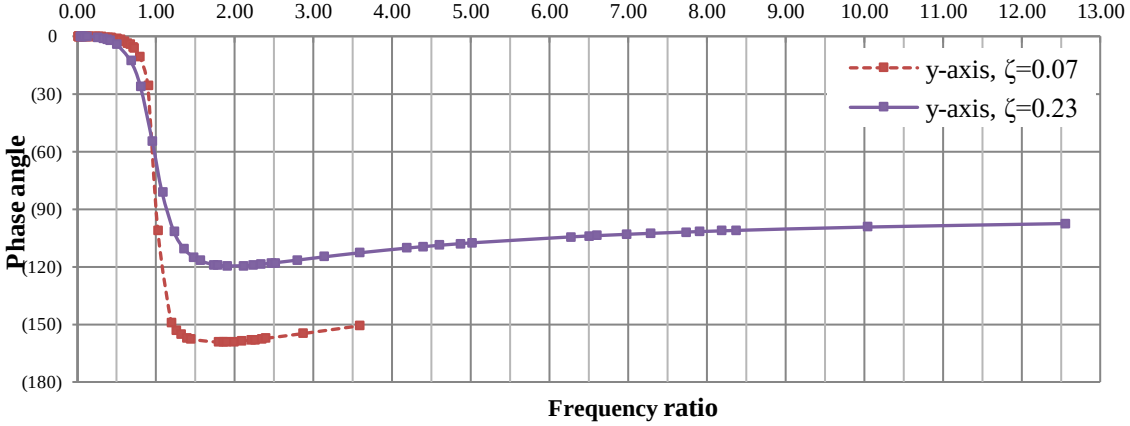

Figure 13. Frequency response curves of 36 kV-circuit breaker in y-axis ((ϕ^1) vs. r)

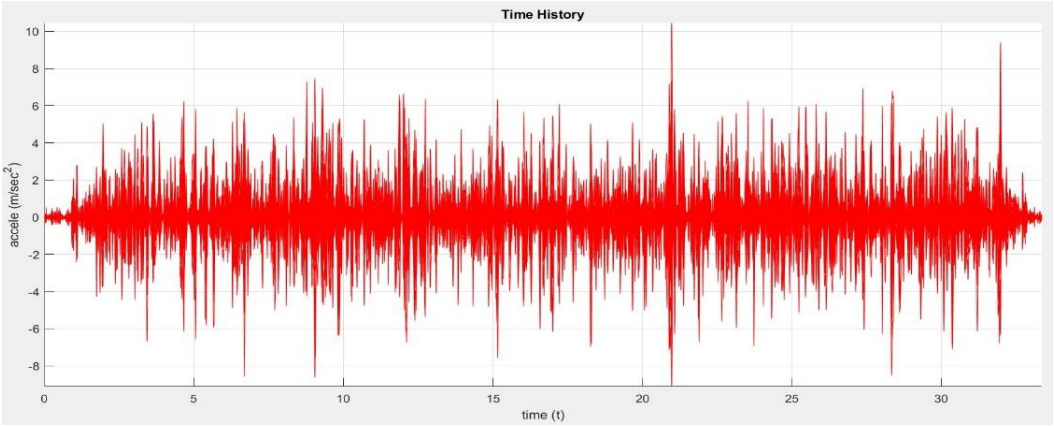

Figure 14. Time history of 36 kV-circuit breaker in x-axis

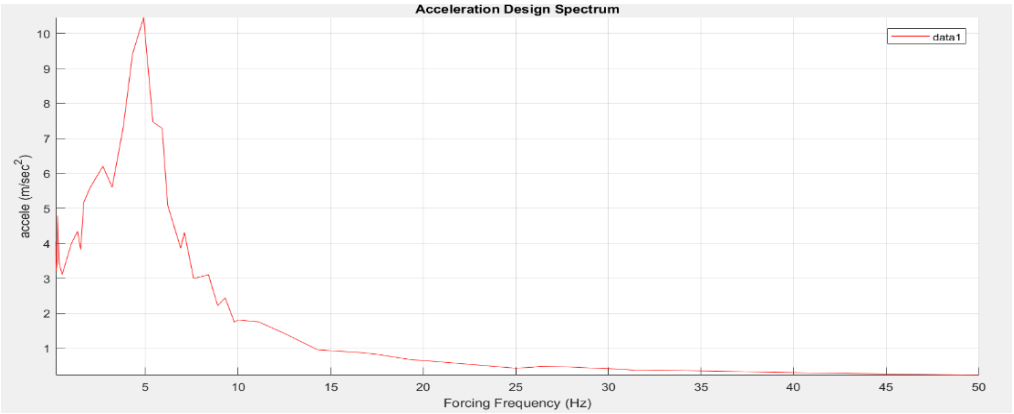

Figure15. Response acceleration spectra of 36 kV-circuit breaker in x-axis

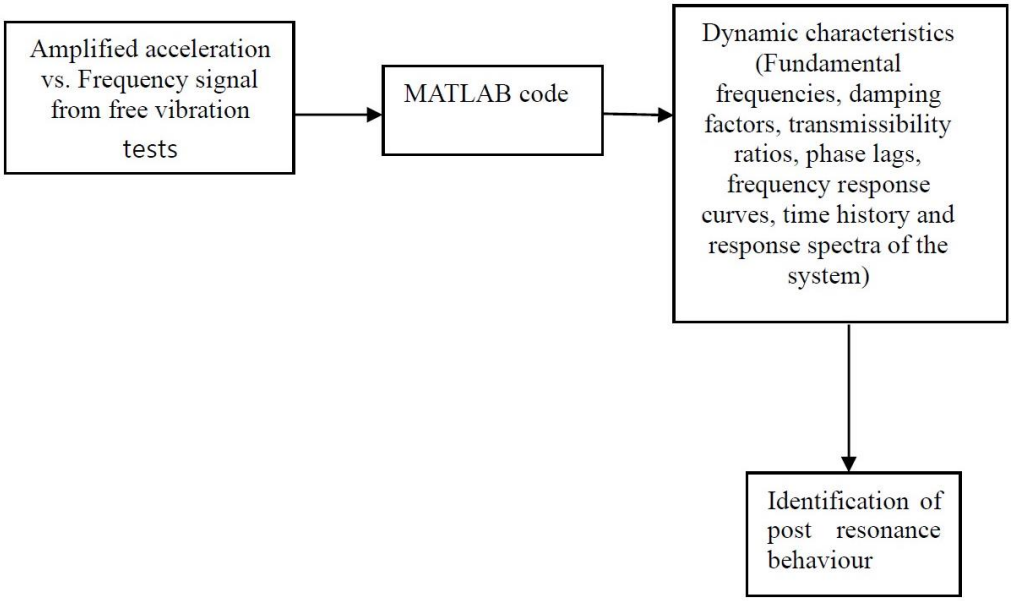

Figure 16. Flow chart representing the proposed method

3. Results and discussions

The frequency response plots related to the acceleration transmission and response phase angles of different electrical systems at first mode are presented. The below discussion follows major findings about the behaviour of electrical power equipment using the plots as shown in Fig. 2(a) and Figs. 10 to 15.

1. For forcing frequency $\omega_0 << $ natural frequency ω_n, under slowly varying forces the group of substation equipment has acceleration transmissibility ≈ 1. Irrespective of damping, all the systems exhibited unit transmissibility at low-frequency levels (Fig. 2(a), Figs. 10 and 12). A rigid movement is exhibited in the mass of the system equally with the support allowing both systems to undergo identical ground motion i.e., absolute motion.

2. At $\omega_0 = \omega_n$, peak acceleration transmission is largely depending on system damping. The transmitted acceleration is maximum relative to the input base excitation at low levels of damping i.e., resonance; therefore, the transmitted excitation. $\frac{\sqrt{(1+(2\zeta r)^2)}}{2\zeta}\ddot{u}_{g0}$. Increase in damping reduces the acceleration transmission. From the Fig. 2(a), with the damping of 0.06, 132 kV CT attained peak transmissibility of 8.0 whereas 245 kV CT with damping 0.26 showed 2.0. The 36 kV CB has achieved transmitted acceleration 3.0 times higher than the input acceleration in x-axis at 0.26 damping and the factor is slightly higher than 2.0 at 0.23 damping in y-axis for the predominant modes.
3. For $\omega_0 \gg \omega_n$, under rapidly varying forces the maximum acceleration transmission $\ddot{u}_o^t$ less than the applied ground acceleration u_{g0} and the factor of transmissibility gradually inclines to zero. At $\left(\frac{\omega_0}{\omega_n}\right) \succ \sqrt{2}$, the equipment with high damping receives comparable transmitted acceleration with the less damped equipment having lesser transmission but non-zero quantity (T_r is still being under 1.0 under both the cases). The equipment 245 kV CT with damping 0.26 has exhibited response of 9.56 m/sec^2. The equipment 132 kV CT with 6% damping has transmission of 0.9 m/sec^2. Second mode of 36 kV CB in x and y axes with 8% and 7% damping also contained less transmission. But the analysis is desired for first and predominant modes of the system. At $\left(\frac{\omega_0}{\omega_n}\right) \succ\succ \sqrt{2}$ (larger frequency ratios), less damped systems (132 kV CT and 300 kV CT) and high damped system (170 kV CT) approaching zero transmissibility. Therefore, the maximum transmitted acceleration $\ddot{u}_t \approx 0$ for any system and is unaffected by the system damping. Which implies the top of the system stays still while the support base beneath it subjected to higher ground accelerations. All the curves beyond the range aiming towards zero transmissibility as ω_0 tends to infinity (ω_n). The discussion continues for the plots of phase angle- frequency ratio as shown in Fig. 2(b) and 11.
4. For all values of $\left(\frac{\omega_0}{\omega_n}\right) \prec\prec 1$, the response lag is close to 0°, transmitted motion is in phase with the ground motion at low excitation frequencies. The acceleration transmission of all systems maintains negligible response lag with the ground motion where both-response and input motions are moving in the same phase and is independent of damping.
5. At systems with $\left(\frac{\omega_0}{\omega_n}\right) \approx 1$, systems with less damping undergo peak response acceleration at phase lag of 90° with the base excitation. Resonance is observed at ϕ^1= 90° in 132 kV CT at 0.06 damping. Decrement in phase thereby reduction in response is observed as damping increases. 245 kV CT and 36 kV CB with 0.26 damping in x-axis has 60° phase lags the applied force recorded at resonance.
6. For all values of $\left(\frac{\omega_0}{\omega_n}\right) \succ 1$, at ϕ^1=180°, system response is out of phase with the base motion giving a definition of instability in the structure. The phase angle of less damped system 132 kV-CT after the resonance is 165°, which allows the equipment to transmit the acceleration under the influence of resonance. At higher levels of forcing frequencies

$\left(\frac{\omega_0}{\omega_n}\right) \succ\succ 1$, the curve progressively shifts upwards to down adopt zero transmission. The less damped systems 132 kV CT and 300 kV CT with the phase difference close to 135° and 120° and largely damped systems 170 kV CT and 36 kV CB has about 105° lag with the induced excitation approaches zero transmission. At the phase angle of 105° with the forcing frequency 49.98 Hz, the response acceleration of 36 kV CB is 0.18 m/sec^2. In general, the maximum permitted value of earthquake forcing frequency 33 Hz, accordingly, the response at 33 Hz is noticed as 0.3 m/sec^2. Similar response behaviour is observed for rest of the equipment. Hence at larger frequency ratios the response of all the equipment is approximately zero and is unchanged by system damping. Therefore, the response of the system is significantly influenced by the response lag depending on the system damping at various frequency levels which is revealed in the plot shown in Fig. 15.

4. Conclusions

Resonance is defined at the forcing frequency where the peak transmission occurred at less damping values and is considered as critical condition in seismic performance of the structure. Therefore, frequency response curves are intended to recognize dynamic response during and after the resonance to envisage the possibility of base isolation in the structure.

1. All equipment considered in the study exhibited rigid movements along with the base accelerations within the range of resonance and is independent of damping. At resonance, the systems reached peak acceleration in their fundamental mode in x-axis and noted that there is a decrement in dynamic transmission with the rise in damping.
2. The transmission/response studies of the system derived several inferences of post resonance behaviour. As discussed earlier, for all $\left(\frac{\omega_0}{\omega_n}\right) \prec\prec \sqrt{2}$, maximum acceleration transmission of all systems $\ddot{u}^t \approx 0$ irrespective of damping. Mass of the system stands still undergoing zero response while the support structure experiencing induced motions. Therefore, it is required to maintain the support system flexible to balance the external accelerations by minimizing the stiffness of the support hence the natural frequency of the system. No damping is desired in this region since higher damping improves the force transmission as frequency ratio tends to infinity. There is another possibility to maintain the system safe and stable in this region is by isolating the ground vibrations transferring to the system.
3. The dynamic response of the system 245 kVCT under Zone V design spectral duration of 6 seconds in the region $\frac{\omega_0}{\omega_n} \succ 1$, ($\omega_0$=49.8 Hz). As a result, the system has not attained zero response acceleration. Hence, the system would be able to perform satisfactorily under support induced motions.
4. The equipment acquired lower transmission (non-zero) at $\frac{\omega_0}{\omega_n} \succ 1$, when relate with the transmission at resonance. Therefore, all systems considered are safe at critical frequencies.
5. Majority of the equipment considered in the study has zero response acceleration at greater

frequency ratios especially in the cases of 132 kV CT, 300 kV CT, 170 kV CT, 145 kV CT and 36 kV CB. Therefore, modifications are needed in the design as discussed above to reduce the peak response accelerations and hence improve the seismic functioning of the structure.

6. The study achieved the objective using the proposed analytical approach by revealing the dynamic behaviour of the structure in the duration of entire seismic signal.
7. The factor of transmissibility values obtained for all the equipment is more than the IEEE standard 693-2005 specified. Hence revision of the standard is highly recommended.
8. The MATLAB code assists users in identifying the tendency of the structure to earthquake vibrations using the quantity of acceleration transmission and phase shift, thereby able to estimate the response spectrum of the structure.

Acknowledgments

The authors gratefully acknowledge the experimental testing support received from Central Power Research Institute, Bangalore, India.

References

1. Schiff, A.J. (2006). IEEE transformer bushing conference subcommittee. IEEE standard 693-2005, IEEE recommended practice for seismic design of substations.
2. Villaverde, R., Pardoen, G.C., Carnalla S. (2001). Ground motion amplification at flange level of bushings mounted on electric substation transformers. Earthquake Engineering and Structural Dynamics, 30(5), 621-632. https://doi.org/10.1002/eqe.26.
3. Ersoy, S., Saadeghvaziri, M.A. (2004). Seismic response of transformer-bushing systems. IEEE Transactions on Power Delivery, 19(1), 131-137. https://doi.org/10.1109/TPWRD.2003.82021.
4. Hatami, M., Ghafory, M., Husseni, M. (2004). Experimental and analytical study of a high voltage instrument transformer. 13th World conference on earthquake engineering, Vancouver, B.C., Canada.
5. Filiatrault, A., Matt, H. (2006). Seismic response of high voltage electrical transformer bushing systems. Journal of Structural Engineering, 132(2), 287-295. https://doi.org/10.1061/(ASCE)0733-9445(2006)132:2(287).
6. Dinh, N.H., Lee, S.J., Kim, J.Y., Choi, K.K. (2020). Study on seismic performance of a mold transformer through shaking table tests. Applied Sciences, 10(1), 361. https://doi.org/10.3390/app10010361.
7. Wen, B., Taciroglu, E., Niu, D. (2015). Shake table testing and numerical analysis of transformer substations including main plant and electrical equipment interaction. Advances in Structural Engineering, 18(11), 1959-1980. https://doi.org/10.1260/1369-4332.18.11.1959.
8. Ullah, N., Ali, S.M., Shahzad, R., Khan, F. (2018). Seismic qualification and time history shake-table testing of high voltage surge arrester under seismic qualification level moderate. Cogent Engineering, 5(1), 1431375. https://doi.org/10.1080/23311916.2018.1431375.
9. Cao, A.T., Tran, T.T., Nguyen, T.H.X., Kim, D. (2020). Simplified approach for seismic risk assessment of cabinet facility in nuclear power plants based on cumulative absolute velocity. Nuclear Technology, 206(5), 743-757. https://doi.org/10.1080/00295450.2019.1696643.
10. Zhu, Z., Zhang, L., Cheng, Y., Guo, H., Lu, Z. (2020). On the nonlinear seismic responses of shock absorber-equipped porcelain electrical components. Mathematical Problems in Engineering, 2020(1), 9026804. https://doi.org/10.1155/2020/9026804.

11. Mohammadi, R.K., Akrami, V., Nikfar, F. (2013). An improvement to seismic design of substation support structures. Structural Engineering and Mechanics, 45(6), 000-000. https://doi.org/10.12989/sem.2013.45.6.821.
12. Kopse, D., Rudez, U., Mihalic, R. (2015). Applying a wide-area measurement system to validate the dynamic model of a part of European power system. Electric Power Systems Research, 119, 1-10. https://doi.org/10.1016/j.epsr.2014.08.024.
13. Orlandini, V., Pierobon, L., Schløer, S., De Pascale, A., Haglind, F. (2016). Dynamic performance of a novel offshore power system integrated with a wind farm. Energy, 109, 236-247. https://doi.org/10.1016/j.energy.2016.04.073.
14. Zareei, S.A., Hosseini, M., Ghafory-Ashtiany, M. (2017). Evaluation of power substation equipment seismic vulnerability by multivariate fragility analysis: a case study on a 420 kV circuit breaker. Soil Dynamics and Earthquake Engineering, 92, 79-94. https://doi.org/10.1016/j.soildyn.2016.09.026.
15. Baghmisheh, A.G., Estekanchi, H.E. (2019). Effects of rigid bus conductors on seismic fragility of electrical substation equipment. Soil Dynamics and Earthquake Engineering, 125, 105733. https://doi.org/10.1016/j.soildyn.2019.105733.
16. Baghmisheh, A.G., Estekanchi, H.E. (2021). Quantifying seismic response uncertainty of electrical substation structures using endurance time method. Structures, 30, 838-849. https://doi.org/10.1016/j.istruc.2021.01.045.
17. Moustafa, M.A., Mosalam, K.M. (2021). Finite element modeling and assessment of seismic response of electrical substations porcelain post insulators. Soil Dynamics and Earthquake Engineering, 150, 106895. https://doi.org/10.1016/j.soildyn.2021.106895.
18. Xie, Q., Shi, G., Liu, Y. (2022). Influence of lumped mass and rotary inertia on seismic isolated post equipment. Journal of Constructional Steel Research, 199, 107604. https://doi.org/10.1016/j.jcsr.2022.107604.
19. Gong, J., Zhi, X., Shao, Y., Dai, K., Zhong, J. (2022). Directionality effect in the seismic fragility of long-span supporting frames in ultrahigh-voltage substation. Soil Dynamics and Earthquake Engineering, 159, 107322. https://doi.org/10.1016/j.soildyn.2022.107322.
20. Fu, Y., Sivaselvan, M.V. (2023). Nonlinear dynamics of short-span electrical conductor cables under uniaxial periodic excitation. Journal of Sound and Vibration, 543, 117319. https://doi.org/10.1016/j.jsv.2022.117319.
21. Ghasemi, H., Farahani, E.S., Fotuhi-Firuzabad, M., Dehghanian, P., Ghasemi, A., Wang, F. (2023). Equipment failure rate in electric power distribution networks: an overview of concepts, estimation, and modeling methods. Engineering Failure Analysis, 145, 107034. https://doi.org/10.1016/j.engfailanal.2022.107034.
22. Arredondo, C., Jaimes, M.A., Reinoso, E. (2019). A simplified model to evaluate the dynamic rocking behavior of irregular free-standing rigid bodies calibrated with experimental shaking-table tests. Journal of Earthquake Engineering, 23(1), 46-71. https://doi.org/10.1080/13632469.2017.1309601.
23. Fu, Z., Tian, L., Luo, X., Pan, H., Liu, J., Liu, C. (2024). Study on the influence of structural and ground motion uncertainties on the failure mechanism of transmission towers. Earthquakes and Structures, 26(4), 311. https://doi.org/10.12989/eas.2024.26.4.311.
24. IS 1893 (Part-1) (2016). Criteria for earthquake resistant design of structures. Part 1: general provisions and buildings (sixth revision). Bureau of Indian Standard.
25. Suresh, L., Mini, K.M. (2019). Effect of multiple tuned mass dampers for vibration control in high-rise buildings. Practice Periodical on Structural Design and Construction, 24(4), 04019031. https://doi.org/10.1061/(ASCE)SC.1943-5576.0000453.
26. Botić, A., Hadzalic, E., Balić, A. (2022). Soil-structure interaction effects on the seismic response of multistory frame structure. Coupled Systems Mechanics, 11(5), 373-387. https://doi.org/10.12989/csm.2022.11.5.373.
27. Lee, S.M., Jeon, B.G., Jung, W.Y. (2024). Seismic performance assessment and reliability verification of molded transformers based on shaking table tests. Earthquakes and Structures, 27(5), 431. https://doi.org/10.12989/eas.2024.27.5.431.

28. Fereidooni, O., Zarfam, P., Mansoori, M. (2025). Mathematical and finite element investigation on time period of coupled steel frames subjected to earthquake excitations. Coupled Systems Mechanics, 14(3), 201-229. https://doi.org/10.12989/csm.2025.14.3.201.
29. Magdy, A., Hammad, A., Shedid, M., Okail, H. (2025). Analytical investigation of seismic response of reinforced concrete coupled shear walls with structural fuses. Earthquakes and Structures, 28(6), 489. https://doi.org/10.12989/eas.2025.28.6.489.
30. Han, M., Gao, X., Zhou, Z., Yang, J. (2026). Seismic performance of base-isolated steel frames considering the influence of rotational ground motions. Earthquakes and Structures, 30(4), 461. https://doi.org/10.12989/eas.2026.30.4.461.
31. Shin, D.H., Eum, Y.C., Kang, S.H., Park, Y., Han, S.J. (2026). Numerical investigations on seismic performance of reinforced concrete columns with corroded rebars. Earthquakes and Structures, 30(1), 61-79. https://doi.org/10.12989/eas.2026.30.1.061.